

Microwave-hydrothermal/solvothermal synthesis of kesterite, an emerging photovoltaic material

Xinlong Yan^{a,c}, Elizabeth Michael^b, Sridhar Komarneni^{c,*}, Jeffrey R. Brownson^d, Zi-Feng Yan^a

^aState Key Laboratory of Heavy Oil Processing, CNPC Key Laboratory of Catalysis, China University of Petroleum, Qingdao 266555, PR China

^bDepartment of Materials Science and Engineering, The Pennsylvania State University, University Park, PA 16802, USA

^cMaterials Research Institute, Materials Research Laboratory, The Pennsylvania State University, University Park, PA 16802, USA

^dDepartment of Energy and Mineral Engineering, The Pennsylvania State University, University Park, PA 16802, USA

Received 1 July 2013; received in revised form 20 July 2013; accepted 21 July 2013

Available online 26 July 2013

Abstract

Rapid synthesis of kesterite ($\text{Cu}_2\text{ZnSnS}_4$), an emerging photovoltaic material was achieved by microwave-hydrothermal/solvothermal (M-H/S) process. Conventional-hydrothermal (C-H) process was also used for comparison with M-H/S process. The synthesized kesterite samples were characterized by powder X-ray diffraction (XRD), scanning electron microscopy (SEM), transmission electron microscopy (TEM) and electron diffraction and UV–vis spectroscopy. Nanophase kesterite, which is potentially suitable for coating was synthesized in ethylene glycol. Band gap values were calculated from UV–vis spectra of several synthetic kesterites and these values are close to the reported values for kesterite.

© 2013 Elsevier Ltd and Techna Group S.r.l. All rights reserved.

Keywords: Kesterite; Microwave-hydrothermal; Microwave-solvothermal; Band gap

1. Introduction

Kesterite $\text{Cu}_2\text{ZnSnS}_4$, or copper zinc tin sulfide (CZTS), is an important emerging semiconducting material that has applications in thin film photovoltaic technologies. It is less commonly exploited for thermoelectric energy harvesting [1], although CZTS could prove to be an interesting material for the transfer of waste heat into electricity. CZTS is a particularly desirable material because it is composed of abundant, environmentally benign elements, and offers advantageous optical and electronic properties. CZTS has an adjustable band gap between 1.45 and 1.51 eV [2], which is optimum for matching the range of solar irradiation.

There is no consensus on the optimal processing method for CZTS. Various techniques, such as atom beam sputtering, thermal evaporation, pulsed laser deposition, and nanocomposite techniques, have been explored with varying degrees of success; processing methods are broadly divided into vacuum and non-vacuum based techniques. Vacuum-based techniques are advantageous because stoichiometry can be very precisely

controlled with high rates of reproducibility, but these approaches limit the scalability of CZTS, as they are energy-intensive with sputtering or evaporation temperatures of 700 °C and annealing temperatures of 500 °C [3]. The most common method for CZTS synthesis is the sequential deposition of zinc, copper, and tin layers, followed by annealing in a sulfur-rich atmosphere. Deposition of these metal layers can occur via thermal evaporation [4], sputtering [3,5], and electrodeposition [6]. Copper-poor, zinc-rich stacks are often employed, as this reduces the formation of copper-containing binary and ternary secondary phases [7,8]. Although these approaches have demonstrated success, with record efficiencies of 10.1% (CZTSe/CZTS materials) [9], improvements are necessary to bring CZTS into the market as a viable thin film absorber for photovoltaics.

Solution-based syntheses of CZTS have been developed to reduce processing time and energy; however, these syntheses require the use of harsh solvents and chemicals. In a typical solution-based synthesis, copper (II) acetylacetonate, zinc acetate, and tin (IV) acetate are combined in an oleylamine solvent and injected into a sulfur and trioctylphosphine oxide solution [10]. Several of these solvents are expensive, unstable, and hazardous, posing health risks and an incompatibility with

*Corresponding author. Tel.: +1 814 865 1542; fax: +1 814 865 2326.

E-mail address: komarneni@psu.edu (S. Komarneni).

the environment. Other volatile organic ligands, such as hydrazine, have been used in similar syntheses [11]. In addition to traditional film deposition techniques, such as spin coating acetate salts in an organic solution and annealing the film in a sulfur-containing atmosphere [12], electrodeposition is thought to be a particularly promising approach due to its low cost, possibility for large area deposition, and room temperature growth [13]. Additionally, nanocomposite techniques have been applied to CZTS processing [14], using binary chalcogenide precursors for synthesis.

To circumvent some of the issues associated with the aforementioned vacuum and non-vacuum based techniques, hydrothermal approaches have been explored. Using the conventional solvothermal technique, nanoparticles of CZTS with diameters of about 5–10 nm were obtained at the temperature of 180 °C by Cao and Shen using a precursor solution containing copper and tin chlorides, zinc acetate, and elemental sulfur in an ethylenediamine solvent. Although CZTS was successfully formed, ZnS also appeared as a secondary phase [15]. Recently one group reported the conventional solvothermal synthesis of metastable orthorhombic CZTS phase using tin dichloride, zinc chloride, copper chloride and thiocarbamide using ethylenediamine and water as solvents at 200 °C for 24 h [16]. They obtained agglomerated powders. Another group recently reported on the synthesis of hydrophilic nanocrystals of CZTS by a modified solvothermal method using tin dichloride, zinc sulfate and copper chloride in ethylene glycol and then developed a film-printing technique based on as-synthesized hydrophilic CZTS ink for fabricating flexible and environmentally friendly CZTS solar cells [17]. Shin et al. [18], Wang et al. [19] and Kumar et al. [20] reported the synthesis of CZTS by using the microwave-assisted solution method. Thus although a few studies used the conventional or microwave solvothermal/hydrothermal route for CZTS synthesis, this technique has not been thoroughly explored, and further work should be done to optimize the synthesis of CZTS using hydrothermal methods. In this work, several hydrothermal and microwave-hydrothermal [21] syntheses were explored, and the resulting powders probed for phase identity, purity, and band gap. The primary focus of the present study was the use of not only microwaves but also the use of optimal sulfur source for CZTS processing, as sulfur is extremely volatile and sulfur-deficient CZTS is a common processing obstacle [22] in addition to phase purity.

2. Experimental section

2.1. Chemicals

Cupric chloride crystals ($\text{CuCl}_2 \cdot 2\text{H}_2\text{O}$) was purchased from Fisher Scientific company. Zinc chloride (>97%) was obtained from BDH Chemicals. Ethylene glycol was purchased from J. T. Baker Chemicals. Tin (II) chloride (98%), glutathione (reduced, 98%) and Polyvinylpyrrolidone (PVP) (Mol. wt. 40,000) were purchased from Sigma-Aldrich company. Ethylenediamine (99%), thioacetamide (98%) and

sodium sulfide were purchased from Alfa Aesar Chemicals. All starting materials were used without further purification.

2.2. Synthesis of $\text{Cu}_2\text{ZnSnS}_4$ nanocrystals by the hydrothermal method

The $\text{Cu}_2\text{ZnSnS}_4$ material was synthesized based on the conventional hydrothermal (C-H) method reported by Jiang et al. [16], but using thioacetamide and glutathione as sulfur sources. Typically, 2 mmol of CuCl_2 , 1 mmol of ZnCl_2 , 1 mmol of SnCl_2 and 4 mmol of thioacetamide or glutathione were dissolved in a 10 mL mixed solvent of water and ethylenediamine (volume ratio=1:1) or 10 mL pure water with vigorous stirring, respectively. Then the mixture was transferred into Teflon-lined stainless steel autoclaves and kept at 200 °C or 180 °C for different times ranging from 4 to 24 h under static conditions. Finally, the precipitates were collected by centrifugation and washed repeatedly with water and ethanol.

The above mixtures were also subjected to microwave-hydrothermal (M-H) treatment. The M-H experiments were performed using MARS5 microwave digestion system (CEM corporation, Matthews, NC). The synthesis was performed under static conditions at 180 °C for 1 h or 2 h using 300 W of microwave power. The solid products were obtained as described above for C-H experiments.

2.3. Synthesis of $\text{Cu}_2\text{ZnSnS}_4$ nanocrystals by the solvothermal method

The $\text{Cu}_2\text{ZnSnS}_4$ material was synthesized based on the conventional solvothermal (C-S) method previously reported by Tian et al. [17], but here we used the M-H method for $\text{Cu}_2\text{ZnSnS}_4$ synthesis. Typically, 0.9 mmol of CuCl_2 , 0.6 mmol of ZnCl_2 , and 0.5 mmol of SnCl_2 were dissolved in 15 ml of ethylene glycol solution containing PVP (0.4 g/mL) or without PVP. Subsequently, another ethylene glycol solution (15 mL) containing 2.4 mmol of Na_2S was added to the above solution. The resulting mixture was subjected to microwave hydrothermal synthesis performed using the above MARS5 microwave digestion system. The synthesis was performed under static conditions at 180 °C for 15 min or 1 h and 160 °C for 1 h using 300 W of microwave power.

2.4. Characterization

X-ray diffraction patterns for the samples were recorded on a Panalytical Xpert PRO X-ray diffractometer with $\text{Cu K}\alpha$ radiation ($\lambda=1.5406 \text{ \AA}$, 45 kV, 40 mA). SEM was performed using a Hitachi S-4800 field emission scanning electron microscope (accelerating voltage: 3.0 kV). TEM was performed with JEOL JEM-2100UHR, operated at 200 kV.

UV–vis characterization of different kesterite samples was done using a Perkin-Elmer Lambda 950 UV/VIS/NIR Spectrophotometer [23]. A 150 mm integrating sphere attachment in diffuse reflectance mode was used for collection of UV–vis spectra. This instrument is accurate over a 250–2500 nm range,

Table 1

CZTS samples prepared by the conventional hydrothermal method with different durations at 200 °C using EDA/water solution.

Sample	Chemicals ^a	Crystallization duration/h	XRD	Band gap (eV)
CZTS	Thioacetamide	24	Orthorhombic or wurtzite	1.25
CZTS	Thioacetamide	8	Orthorhombic or wurtzite	
CZTS	Thioacetamide	4	Orthorhombic or wurtzite	
CZTS	Thioacetamide	2	Kesterite	
CZTS	Thioacetamide	1	Kesterite+impurity	
CZTS	Glutathione	24	Orthorhombic or wurtzite	
CZTS	Glutathione	8	Orthorhombic or wurtzite	
CZTS	Glutathione	4	Orthorhombic or wurtzite	
CZTS	Glutathione	2	Kesterite	
CZTS	Glutathione	1	Kesterite	

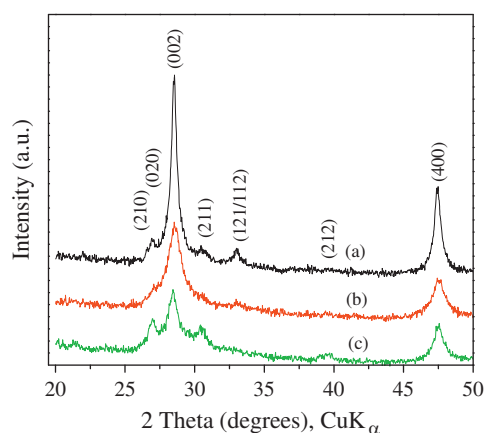
^aCuCl₂, ZnCl₂ and SnCl₂ are the metal sources in all syntheses.

Fig. 1. CZTS samples prepared by the conventional hydrothermal method using water/EDA solution and thioacetamide as the sulfide source: (a) CZTS/200/24, (b) CZTS/200/8 and (c) CZTS/200/4 (peaks correspond to orthorhombic or wurtzite phase).

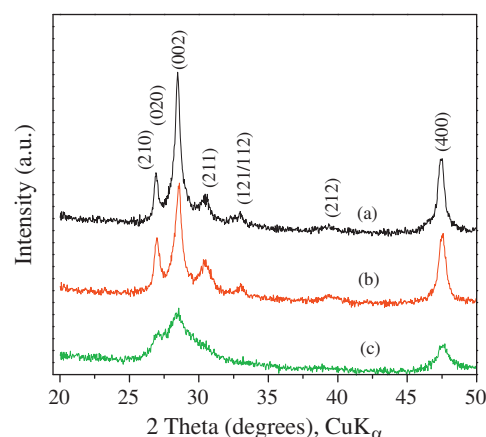


Fig. 2. CZTS samples prepared by the conventional hydrothermal method using water/EDA solution and glutathione as the sulfide source: (a) CZTS/200/24, (b) CZTS/200/8 (c) and CZTS/200/4 (peaks correspond to orthorhombic or wurtzite phase).

but here we used a scan range of 600–1200 nm for collecting UV–vis spectra. The scan range was expanded midway through data collection to encompass a range of 500–1500 nm using a step size of 2 nm. A photomultiplier tube was used as the detector in the ultraviolet and visible regions of the scan range while PbS was used in the near infrared region [23].

3. Results and discussion

3.1. CZTS syntheses by different methods

Table 1 presents the results of CZTS syntheses at 200 °C as a function of time using thioacetamide or glutathione as a sulfur source. Powder XRD results revealed that orthorhombic or wurtzite CZTS phases were obtained when treated for 4 or more hours with thioacetamide or glutathione as the sulfide source (Figs. 1 and 2) while kesterite phase was detected after 1–2 h of reaction (Table 1). The peaks of kesterite reported above matched with Joint Committee on Powder Diffraction Standards (JCPDS) card No. 26-0575 for kesterite CZTS. Orthorhombic phase was reported as a metastable phase

previously using thiocarbamide as sulfide source with ethylenediamine and water as solvents at 200 °C for 24 h [16]. Our results here with 1–2 h of treatment time resulted in kesterite but prolonged treatment led to orthorhombic phase (Table 1) using thioacetamide or glutathione as a sulfur source. Earlier studies [16] reported results for only 24 h of treatment time where orthorhombic phase formed and hence they did not report on the formation of kesterite CZTS phase. Scanning electron micrographs of samples prepared at 200 °C/24 h by the C-H method using water/EDA solution of CuCl₂, ZnCl₂ and SnCl₂ as the metal sources and thioacetamide as the sulfide source showed aggregated nanoparticles (Fig. 3a) as has been reported earlier [16]. However, when glutathione was used as the sulfide source the aggregation of nanoparticles appear to be massive (Fig. 3b).

Table 2 presents the results of CZTS syntheses using water as the only solvent and CuCl₂, ZnCl₂ and SnCl₂ as the metal sources with thioacetamide as the sulfide source. Both conventional and microwave hydrothermal methods were used for CZTS syntheses using the above precursors. The results obtained clearly show that kesterite CZTS formed in all cases (Table 2) as the peaks matched with JCPDS card No. 26-0575

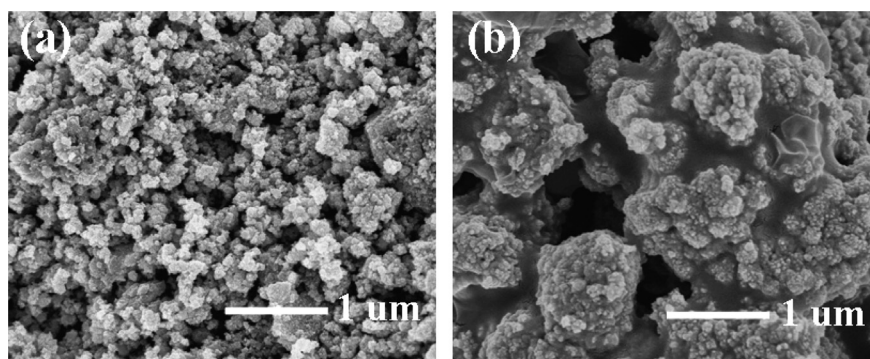


Fig. 3. SEM pictures of samples prepared at 200 °C/24 h by the C-H method using water/EDA solution of CuCl₂, ZnCl₂ and SnCl₂ as the metal sources and thioacetamide as the sulfide source (a) or glutathione as the sulfide source (b).

Table 2

CZTS samples prepared by conventional and microwave hydrothermal methods with different durations using water solution.

Sample ^a	Crystallization		XRD	Band gap (eV)
	Temperature/°C	Duration/h		
CZTS	200	24	Kesterite	
CZTS	180	24	Kesterite	1.50
CZTS	180	8	Kesterite	1.45
CZTS	180	4	Kesterite	1.40
CZTS ^b	180	1	Kesterite	1.60
CZTS ^b	180	2	Kesterite	1.50

^aCuCl₂, ZnCl₂ and SnCl₂ are the metal sources and thioacetamide is the sulfide source in all syntheses.

^bThese two samples were prepared by the microwave hydrothermal method, while other samples were prepared by the conventional method.

for kesterite CZTS. Fig. 4 shows the XRD patterns of kesterite prepared using the conventional hydrothermal method at 180 °C for 24, 8 and 4 h (Fig. 4a, b and c, respectively). There is little or no change in crystallinity as a function of time as all the XRD peaks are similar in breadth and intensity using the conventional hydrothermal method (Fig. 3). Microwave-hydrothermal method, on the other hand, yielded kesterite after 1 h of treatment and the XRD peaks closely matched with those prepared by the conventional method in peak breadth and intensity. These crystallization studies are supported by previous studies which indicated that after nucleation, crystal growth is controlled by both thermodynamics and kinetics [24], thermodynamic factors are from crystallographic limits, while kinetic factors are determined by varying conditions depending upon different systems [25]. The above results suggest that kesterite could be made more rapidly by the microwave-hydrothermal method than by the conventional method confirming previous results of faster kinetics of crystallization with microwave-assisted methods [21,26,27]. Scanning electron micrographs of kesterite clearly show aggregated nanoparticles under both C-H and M-H conditions (Fig. 5). However, it is interesting to note that rod-like morphologies were observed at shorter durations of hydrothermal treatment under both C-H and M-H conditions (Fig. 5c, d and e, see lower magnifications). These rod-like structures were converted to nanoparticle aggregates of kesterite as can be seen with the inset in Fig. 5c shown at higher

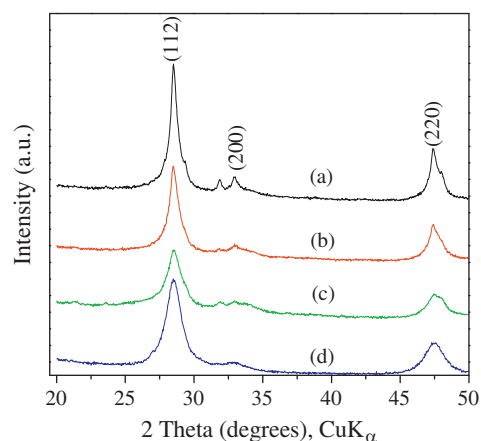


Fig. 4. CZTS samples prepared by the conventional or microwave hydrothermal method by using water solution of CuCl₂, ZnCl₂ and SnCl₂ as the metal sources and thioacetamide as the sulfide source: (a) CZTS-CH-180-24 h, (b) CZTS-CH-180-8 h, (c) CZTS-CH-180-4 h and (d) CZTS-MH-180-1 h (peaks match with CZTS, JCPDS 26-0575).

magnification. Thus the morphology of kesterite is aggregated nanoparticles which showed broad diffraction peaks (Fig. 4).

3.2. Nanocrystals of CZTS using the M-H method

We used the M-H method here for the first time to synthesize nanocrystals of kesterite using an already reported

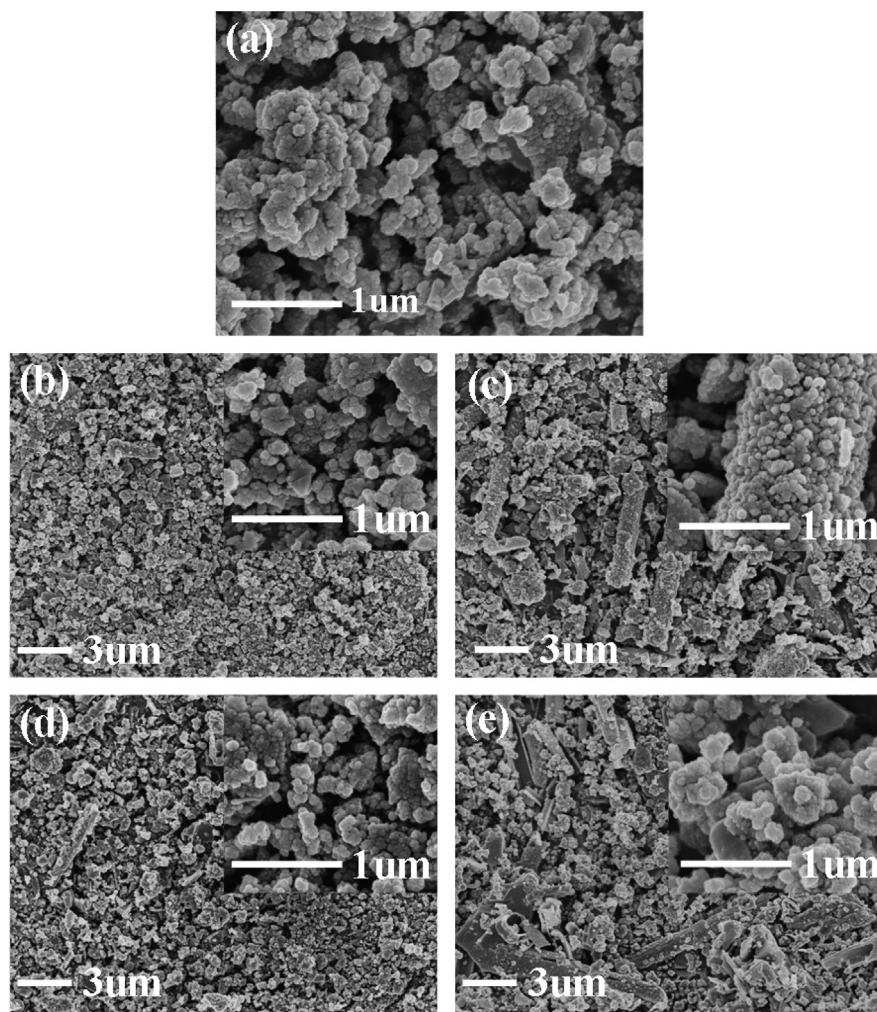


Fig. 5. SEM pictures of CZTS samples prepared by conventional hydrothermal (C-H) and microwave-hydrothermal (M-H) methods with different durations using water solution of CuCl_2 , ZnCl_2 and SnCl_2 as the metal sources and thioacetamide as the sulfide source: CZTS-CH-200-24 h (a), CZTS-CH-180-24 h (b), CZTS-CH-180-8 h (c), CZTS-CH-180-4 h (d), and CZTS-MH-180-1 h (e).

Table 3

CZTS samples prepared by the microwave hydrothermal method at different temperatures and durations of treatment using ethylene glycol solution.

Sample	Chemicals ^a	Crystallization		XRD	Band gap (eV)
		Temperature/°C	Duration		
CZTS	Na_2S , PVP	180	15 min	Kesterite	1.30
CZTS	Na_2S , PVP	180	1 h	Kesterite	1.30
CZTS	Na_2S , PVP	160	1 h	Kesterite	1.25
CZTS	Na_2S , without PVP	180	15 min	Kesterite	1.15
CZTS	Na_2S , without PVP	180	1 h	Kesterite	1.15
CZTS	Na_2S , without PVP	160	1 h	Kesterite	1.30

^a CuCl_2 , ZnCl_2 and SnCl_2 are the metal sources in all syntheses.

conventional-solvothermal method [17]. Our objective here is to make kesterite nanoparticles for coating large areas using a cheaper, greener and faster M-H method for synthesis. Table 3 shows the results of kesterite syntheses using chloride salts of Cu, Zn and Sn with Na_2S and ethylene glycol and with and

without polyvinylpyrrolidone (PVP). Kesterite phase (the peaks matched with JCPDS card No. 26-0575 for kesterite CZTS) was synthesized in as little a time as 15 min at 180 °C and in 1 h at 160 °C (Table 3). Powder XRD results suggested nanoparticle size with and without PVP as the peaks are very

broad (Fig. 6). TEM results of morphology (Fig. 7) and electron diffraction (inset, Fig. 7a) confirmed the nanocrystals of kesterite. Lattice fringe images shown as insets also confirm kesterite formation with 3.1 Å spacing.

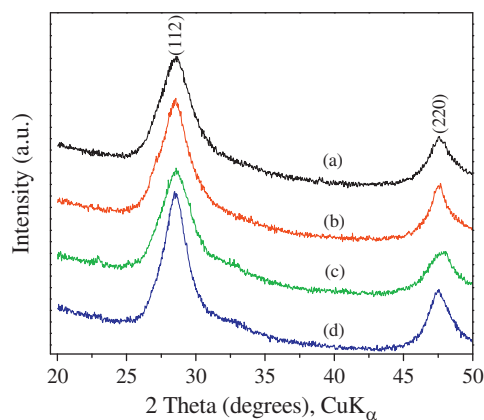


Fig. 6. CZTS samples prepared by the microwave hydrothermal method with and without PVP using ethylene glycol solution: (a) CZTS-MH-160-1 h, (b) CZTS-MH-180-1 h, (c) CZTS-MH-without PVP-160-1 h and (d) CZTS-MH-without PVP-180-1 h (peaks match with CZTS, JCPDS 26-0575).

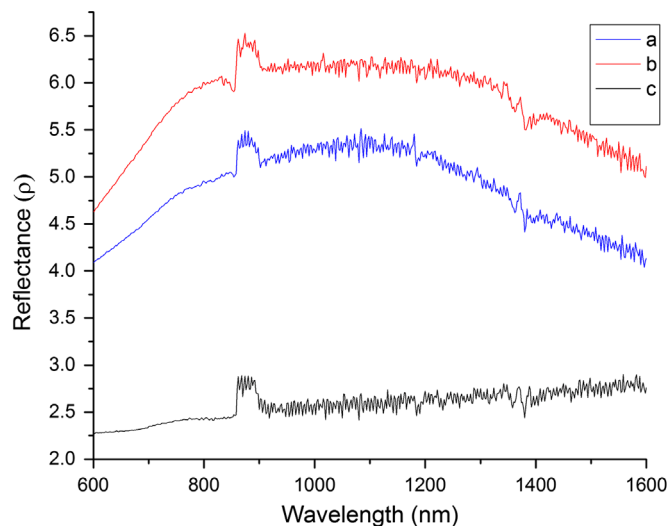


Fig. 8. UV-vis spectra of CZTS samples prepared by the conventional hydrothermal method at 180°C/24 h (a) and the microwave hydrothermal method at 180 °C/2 h using water solution of CuCl_2 , ZnCl_2 and SnCl_2 and thioacetamide and CZTS sample prepared by the microwave hydrothermal method at 160 °C/1 h using ethylene glycol solution of Na_2S , CuCl_2 , ZnCl_2 and SnCl_2 without PVP (c).

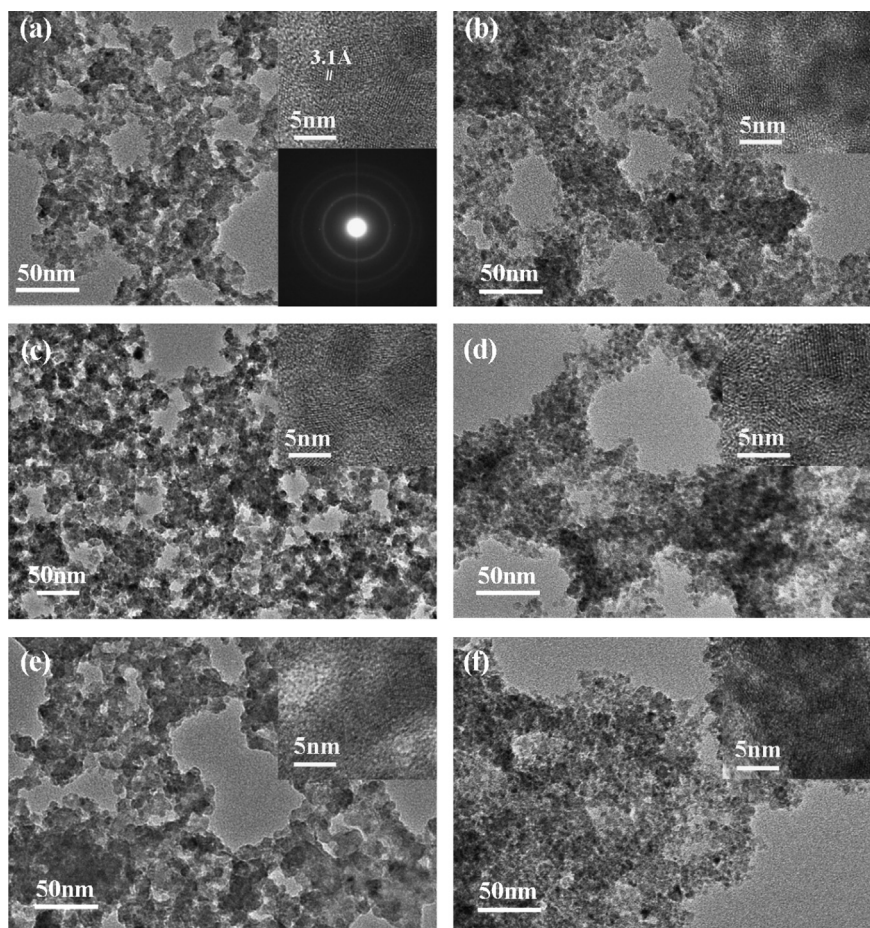


Fig. 7. TEM images of CZTS samples prepared by the microwave hydrothermal method with and without PVP using ethylene glycol solution: (a) CZTS-MH-160-1 h, (b) CZTS-MH-without PVP-160-1 h, (c) CZTS-MH-180-15 min, (d) CZTS-MH-without PVP-180-15 min, (e) CZTS-MH-180-1 h and (f) CZTS-MH-without PVP-180-1 h.

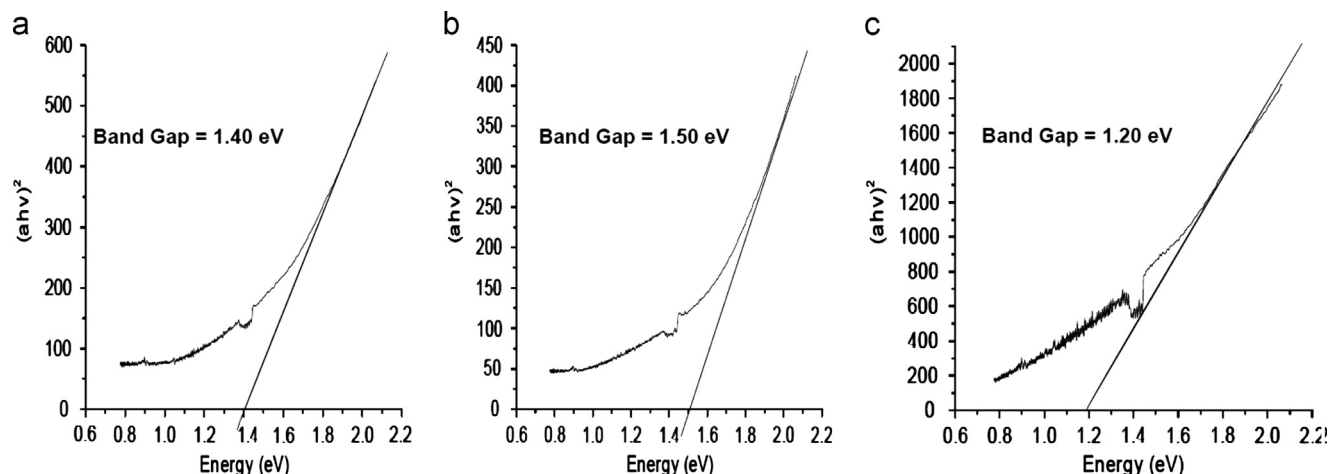


Fig. 9. Band gap values of CZTS samples prepared by conventional-hydrothermal method at 180 °C/24 h (a) and microwave-hydrothermal method at 180 °C/2 h using water solution of CuCl_2 , ZnCl_2 and SnCl_2 and thioacetamide and CZTS sample prepared by microwave hydrothermal method at 160 °C/1 h using ethylene glycol solution of Na_2S , CuCl_2 , ZnCl_2 and SnCl_2 without PVP (c).

3.3. UV-vis spectra and band gap values of CZTS

Fig. 8 shows the UV-vis diffuse reflectance spectra of three different kesterite samples prepared by three different methods. The band gaps of the above three kesterite samples calculated from Kubelka–Munk transformations are shown in Fig. 9 as examples. The determined band gaps of the differently prepared kesterites are in the range of 1.15–1.55 (Tables 1, 2 and 3) compared to the anticipated bandgaps of 1.5 for the bulk CZTS material [28]. The best match with theoretical band gap of kesterite was obtained with CZTS samples prepared by conventional and microwave hydrothermal methods with different durations using water solution of CuCl_2 , ZnCl_2 and SnCl_2 as the metal sources and thioacetamide as the sulfide source (Table 2). This is probably because of larger size crystals obtained by this method (Fig. 5). The small differences in band gap values between the experimentally determined values and the theoretical values could be explained by the smaller crystal sizes as has been shown previously for a different material [28]. Note that the smallest band gaps were obtained for nanocrystals of kesterite (Fig. 7) materials synthesized in ethylene glycol (Table 3). However, further studies are needed to optimize the band gap values of some of the kesterites synthesized here.

4. Conclusions

Both the microwave-hydrothermal/solvothermal (M-H/S) process and the conventional-hydrothermal (C-H) process were used successfully for kesterite synthesis using different precursors. Nanophase kesterites were synthesized by both M-H and C-H processes in ethylene glycol which showed band gap values in the range of 1.4–1.6.

Acknowledgement

The senior author (XY) thanks CSC for financial support.

References

- [1] H. Yang, L.A. Jauregui, G. Zhang, Y.P. Chen, Y. Wu, Nontoxic and abundant copper zinc tin sulfide nanocrystals for potential high-temperature thermoelectric energy harvesting, *Nano Letters* 12 (2012) 540–545.
- [2] B. Silvana, D. Kammerlander, Miguel A.L. Marques, Band structures of $\text{Cu}_2\text{ZnSnS}_4$ and $\text{Cu}_2\text{ZnSnSe}_4$ from many-body methods, *Applied Physics Letters* 98 (2011) 241915–241918.
- [3] A.J. Cheng, M. Manno, A. Khare, C. Leighton, S.A. Campbell, E.S. Aydil, Imaging and phase identification of $\text{Cu}_2\text{ZnSnS}_4$ thin films using confocal Raman spectroscopy, *Journal of Vacuum Science and Technology A* 29 (2011) 051203–051214.
- [4] K. Gunawan Wang, O. Todorov, T. Shin, B. Chey, S.J. Bojarczuk, N. Mitzi, A.D. Guha, S., Thermally evaporated $\text{Cu}_2\text{ZnSnS}_4$ solar cells, *Applied Physics Letters* 96 (2010) 143508–143511.
- [5] S. Jae-Seung, S.Y. Lee, J.C. Lee, H.D. Nam, K.H. Kim, Electrical and optical properties of $\text{Cu}_2\text{ZnSnS}_4$ thin films prepared by rf magnetron sputtering process, *Solar Energy Materials and Solar Cells* 75 (2003) 155–162.
- [6] J.J. Scragg, D.M. Berg, P.J. Dale, A 3.2 percent efficient kesterite device from electrodeposited stacked elemental layers, *Journal of Electroanalytical Chemistry* 646 (2010) 52–59.
- [7] H. Katagiri, K. Jimbo, W.S. Maw, K. Oishi, M. Yamazaki, H. Araki, A. Takeuchi, Development of CZTS-based thin film solar cells, *Thin Solid Films* 517 (2009) 2455–2460.
- [8] Q. Guo, G.M. Ford, W.C. Yang, B.C. Walker, E.A. Hillhouse Stach, R.H.W. Agrawal, Fabrication of 7.2 percent efficient cztsse solar cells using CZTS nanocrystals, *Journal of the American Chemical Society* 132 (2012) 17384–17386.
- [9] D.A.R. Barkhouse, O. Gunawan, T. Gokmen, T.K. Todorov, D.B. Mitzi, Device characteristics of a 10.1% hydrazine-processed $\text{Cu}_2\text{ZnSn}(\text{Se},\text{S})_4$ solar cell, *Progress in Photovoltaics Research and Application* 20 (2011) 6–11.
- [10] S.C. Riha, A.L. Prieto, B.A. Parkinson, Solution-based synthesis and characterization of $\text{Cu}_2\text{ZnSnS}_4$ nanocrystals, *Journal of the American Chemical Society* 131 (2009) 12054–12055.
- [11] T.K. Todorov, K.B. Reuter, D.B. Mitzi, High-efficiency solar cell with earth-abundant liquid-processed absorber, *Advanced Energy Materials* 22 (2010) 156–159.
- [12] K. Tanaka, Y. Fukui, N. Moritake, H. Uchiki, Chemical composition dependence of morphological and optical properties of $\text{Cu}_2\text{ZnSnS}_4$ thin films deposited by sol–gel sulfurization and $\text{Cu}_2\text{ZnSnS}_4$ thin film solar cell efficiency, *Solar Energy Materials and Solar Cells* 95 (2011) 838–842.

- [13] J.J. Scragg, P.J. Dale, L.M. Peter, Towards sustainable materials for solar energy conversion: preparation and photoelectrochemical characterization of $\text{Cu}_2\text{ZnSnS}_4$, *Electrochemistry Communications* 10 (2008) 639–642.
- [14] Y. Wang, H. Gong, Low temperature synthesized quaternary chalcogenide $\text{Cu}_2\text{ZnSnS}_4$ from nano-crystallite binary sulfides, *Journal of the Electrochemical Society* 158 (2011) 800–803.
- [15] M. Cao, Y. Shen, A mild solvothermal route to kesterite quaternary $\text{Cu}_2\text{ZnSnS}_4$ nanoparticles, *Journal of Crystal Growth* 318 (2011) 1117–1120.
- [16] H. Jiang, P. Dai, Z. Feng, W. Fan, J. Zhan, Phase selective synthesis of metastable orthorhombic $\text{Cu}_2\text{ZnSnS}_4$, *Journal of Materials Chemistry* 22 (2012) 7502–7506.
- [17] Q. Tian, X. Xu, L. Han, M. Tang, R. Zou, Z. Chen, M. Yu, J. Yang, J. Hu, Hydrophilic $\text{Cu}_2\text{ZnSnS}_4$ nanocrystals for printing flexible, low-cost and environmentally friendly solar cells, *CrystEngComm* 14 (2012) 3847–3850.
- [18] S.W. Shin, J.H. Han, C.Y. Park, A.V. Moholkar, J.Y. Lee, J.H. Kim, Quaternary $\text{Cu}_2\text{ZnSnS}_4$ nanocrystals: facile and low cost synthesis by microwave-assisted solution method, *Journal of Alloys and Compounds* 516 (2013) 96–101.
- [19] W. Wang, H. Shen, X. He, Study on the synthesis and formation mechanism of $\text{Cu}_2\text{ZnSnS}_4$ particles by microwave irradiation, *Materials Research Bulletin* 48 (2013) 3140–3143.
- [20] R.S. Kumar, B.D. Ryu, S. Chandramohan, J.K. Seol, S.K. Lee, C.H. Hong, Rapid synthesis of sphere-like $\text{Cu}_2\text{ZnSnS}_4$ microparticles by microwave irradiation, *Materials Letters* 86 (2012) 174–177.
- [21] S. Komarneni, R. Roy, Q.H. Li, Microwave-hydrothermal synthesis of ceramic powders, *Materials Research Bulletin* 27 (1992) 1393–1405.
- [22] N. Nakayama, K. Ito, Sprayed films of stannites $\text{Cu}_2\text{ZnSnS}_4$, *Applied Surface Science* 92 (1996) 171–175.
- [23] X. Yan, E. Michael, S. Komarneni, J.R. Brownson, Z.-F. Yan, Microwave- and conventional-hydrothermal synthesis of CuS , SnS and ZnS : optical properties, *Ceramics International* 39 (2013) 4757–4763.
- [24] D. Xue, K. Li, J. Liu, C. Sun, K. Chen, Crystallization and functionality of inorganic materials, *Materials Research Bulletin* 47 (2012) 2838–2842.
- [25] K. Chen, D. Xue, Nanoparticles via crystallization: a chemical reaction control study of copper oxides, *Nanoscience and Nanotechnology Letters* 4 (2012) 1–12.
- [26] S. Komarneni, R. Roy, Titania gel spheres by a new sol–gel process, *Materials Letters* 3 (1985) 165–167.
- [27] S. Komarneni, Q. Li, K.M. Stefansson, R. Roy, Microwave-hydrothermal processing for synthesis of electroceramic powders, *Journal of Materials Research* 8 (1993) 3176–3183.
- [28] C. Persson, Electronic and optical properties of $\text{Cu}_2\text{ZnSnS}_4$ and $\text{Cu}_2\text{ZnSnSe}_4$, *Journal of Applied Physics* 107 (2010) 53710–53718.